*Exp. Theo. NANOTECHNOLOGY* 3 (2019) 61–70 https://doi.org/10.56053/3.1.61

# $TiO_2/Bi_5O_7I$ nanocomposite for photoanode of electrochemical cell

*Anissa A. Putri*[1,2,*], *S. Kato*[1], *N. Kishi*[1], *T. Soga*[1]

[1]Department of Electrical and Mechanical Engineering, Nagoya Institute of Technology, 466-8555 Japan
[2]Chemistry Department, Walisongo State Islamic University, 50185, Indonesia
[*)] E-mail: anissaputri@walisongo.ac.id

*Received* 18/8/2018, *Accepted* 25/12/2018, *Accepted* 15/1/2019

$Bi_5O_7I$ is one of the bismuth oxyiodide (BiOI) derivate with bismuth and oxygen-rich contained which can act as semiconductor material. Here, we reported that a successful $TiO_2/Bi_5O_7I$ nanocomposite films fabrication could be carried out by the annealing treatment of $TiO_2$/BiOI films at 450 °C. The prepared films have been applied as the photoanode in photovoltaic devices by adapting the dye-sensitized solar cell (DSSC) model. Our annealed BiOI was $Bi_5O_7I$ which was proven by the X-Ray diffraction (XRD) patterns of both materials. The usage of $Bi_5O_7I$ in $TiO_2/Bi_5O_7I$ films could change the optical behavior of films which has been indicated by the decreasing in its band gap energy, extending the absorption wavelength edge of the films. The backscattered scanning electron microscope (SEM) images depicted the incorporation of $Bi_5O_7I$ in the $TiO_2$-contained films. We designed the photovoltaic device structure as the arrangement: FTO/$TiO_2$/$Bi_5O_7I$/Iodine electrolyte/Pt-FTO. Overall, the addition of $Bi_5O_7I$ could enhance the photovoltaic performance of $TiO_2/Bi_5O_7I$ cells in comparison to the only $TiO_2$ films. The slight enhancement in short-circuit current values over the $TiO_2/Bi_2O_3$ from the previous report can be the evidence that $Bi_5O_7I$ is also has the benefit which is not only for photocatalytic reaction, but also the photovoltaic application.

**Keywords:** BiOI; $Bi_5O_7I$; $TiO_2$; Nanocomposite; Photovoltaic; Annealing.

## 1. INTRODUCTION

Solar cell device development is still being the most interested research focus among the researchers since the demand of energy has increased rapidly. Solar energy is abundant and it can be considered as the clean renewable resources to generate the electricity [1]. Since the two decades, DSSC has attracted the attention despite the fact on its less stability and high-cost issue. Thus, many researches have been focused to build a competitive photoelectric cell from its performance and its production cost. Although each part in the solar energy device plays an

important role, the photoanode development study has been frequently attempted to achieve the higher power conversion efficiency (PCE). Generally, the photoanode composition in DSSC can be consisted of the semiconductor material and dye. The most common semiconductor materials used in DSSC are $TiO_2$ and ZnO due to

their transparency character, stability in air, and their unique electronic property. However, both the aforementioned materials only can show the higher activity under the UV-Visible light which is only 4% from the reached total solar energy to the earth [2]. To increase the activity of $TiO_2$ and ZnO, some procedures have been developed, like contacting these materials with the dye [3,4].

Another way to improve the $TiO_2$ performance is by sensitization with visible light active photocatalyst to enhance the solar light absorption of $TiO_2$ [5]. The combination of $TiO_2$ with photocatalyst material can affect the band gap energy of semiconductor, the position of valence band and conduction band, and it may have the influence on the both materials crystal form. As a result, the combined semiconductor had the better performance [6,7]. The sensitization of inorganic material in $TiO_2$ or ZnO has some advantages over the dye sensitization. In DSSC, the stability is still being the issue since the organic dye used in this system is mostly unstable [8]. Thus, in line with the previous work [9], we have tried combining $TiO_2$ and bismuth-based material, like $Bi_5O_7I$ to study the bismuth-based material chance for photovoltaic application. In this study, we reported the fabrication of $Bi_5O_7I$ as the bismuth-based material for photovoltaic application without involving the dye in the devices and to the best our knowledge, $Bi_5O_7I$ is no longer applied in photovoltaic devices.

$Bi_5O_7I$ is one of the BiOI families which have the character as semiconductor material and photocatalyst. Due to that fact that it has been common to apply this material as the photocatalyst, it can be considered as the promising material. In photocatalytic reaction, $Bi_5O_7I$ has succeed to degrade the dye, like RhB in water and acetaldehyde [10,11] and phenol [12]. In addition, it is possible to synthesize doped material into $Bi_5O_7I$ and this work could show the performance enhancement of $Bi_5O_7I$ in the photocatalytic reaction [13]. $Bi_5O_7I$ material consists of Bi atom which has the 6s orbital, O atom with its 2p orbital, and 5p orbital from I atom to construct the top of valence bond in $Bi_5O_7I$, while the 6p orbital from Bi atom will exist in its conduction band [14,15]. By this arrangement, the hybridization among 6s orbital and 2p orbital with 5p orbital in the valence band causes the valence band be more dispersed. As a consequence, it allows the photo-generated holes migration [16]. Compared to BiOI, $Bi_5O_7I$ also has the ability in photocatalytic reaction due to the changing in its band gap energy and reduction/oxidation potential in its conduction and valence band as the effect of reducing in the iodine content [17].

Although the low performance of photovoltaic cell is being the problem in our $TiO_2/Bi_5O_7I$ cell, it is interesting to note that due to its narrower band gap energy than $Bi_2O_3$, it could achieve a better Jsc over the $TiO_2$-$Bi_2O_3$ photoanode, 0.341 $mA/cm^2$ [9]. We expect that there will be a chance to improve the bismuth-based value for photovoltaic cell in the future since bismuth has been considered as the potential candidate to replace the lead usage in the photoelectrochemical cell.

## 2. EXPERIMENTAL

### *2.1. $TiO_2/Bi_5O_7I$ nanocomposite film preparation*

$Bi_5O_7I$ was derived from BiOI which was synthesized from 2 mmol of $Bi(NO_3)_3.5H_2O$ and KI precursors. The mixing of precursor for 15 min that was followed by 5 h stirring in 40 mL water prompted the orange mixture as powder material, BiOI. The precipitated then was separated from its solvent and this step was followed by washing in ethanol and water for several times. To prepare $TiO_2$/BiOI nanocomposite films, each of $TiO_2$/BiOI dispersion with percentage of BiOI: 0%; 6.25%; 12.5%; 25%; and 100% was carried out for 15 minutes. Prior to the annealing treatment of $TiO_2$/BiOI films at 450 $^oC$ to obtain $TiO_2/Bi_5O_7I$ films, a doctor blade method was utilized to prepare the films. Around 6 μm of thickness was also detected by cross-sectional SEM image.

### *2.2. Characterization*

To characterize the film properties, we used some instruments to investigate the character of prepared $TiO_2/Bi_5O_7I$ films. X-Ray diffraction (XRD) analysis, RINT-2100 diffractometer was operated to study the structural property of $TiO_2$, BiOI, and $Bi_5O_7I$ films. Scanning electron microscope, FESEM JEOL JSM-7100F was utilized to study the morphology of films. UV-Visible spectrophotometer (JASCO 670 UV) was used to study the optical property of films. Then, for measuring the I-V performance of films, a solar simulator (AM 1.5G, 100 $mW/cm^2$) was involved in our work.

### *2.3. Devices fabrication*

To prepare the photovoltaic devices, we adapted DSSC model in our cell. However, in this work, the films were not soaked into dye solution. The cell consisted of FTO-$TiO_2/Bi_5O_7I$ as photoanode was paired with Pt-FTO as a counter electrode. The iodine electrolyte was interleaved between the active electrodes. The active area for measurement was set up for 0.16 $cm^2$ and the device is illustrated in Fig. 4.

## 3. RESULTS AND DISCUSSION

Here we display the XRD patterns of $TiO_2$, $Bi_5O_7I$ as the result of annealing at 450 $^oC$, and BiOI as the parent bismuth material in our work. The diffractogram is shown in Figure 1. As the annealing process applied, we can see a totally different of structural property between BiOI and $Bi_5O_7I$. BiOI has the (002); (102); and (110) peaks as the character of BiOI which those crystal planes exist in 2θ around 19.6$^o$; 29.8$^o$; and 31.7$^o$, respectively. This BiOI character is in line to the JCPDS card of BiOI no. 73-2062 [18]. In addition, the shifting peak to 2θ 28.2$^o$ and 31.2$^o$ indicates the crystal plane of $Bi_5O_7I$ (312) and (004) which appears in the diffractogram of $Bi_5O_7I$. The analysis of $Bi_5O_7I$ refers to the JCPDS card no 40-0548 and our $Bi_5O_7I$ character has the agreement with the previous report [19]. Since there is no BiOI peak assigned in the $Bi_5O_7I$ diffractogram, we believed that the heating treatment can be a successful way for converting BiOI to $Bi_5O_7I$. The material changing from BiOI to $Bi_5O_7I$ may occur based on the written reaction in Eq. 1. Annealing treatment supported with air oxidation allows the deiodination reaction in BiOI to form the bismuth and oxygen-rich material, like $Bi_5O_7I$.

$$5BiOI + O_2 \rightarrow Bi_5O_7I + 2I_2 \quad (1)$$

Fig. 1 also represents the diffractogram which shows the $TiO_2$ P25 peak character. (101) and (110) crystal planes correspond to anatase (25.2°) and rutile (27.4°) phases [20,21]. By this result, we can differentiate between anatase and rutile phase in $TiO_2$ since both peaks do not overlap. From the d-spacing calculation, we obtained 0.30 nm; 0.316 nm; and 0.353 nm for tetragonal BiOI, orthorhombic $Bi_5O_7I$, anatase $TiO_2$ which indicate the (102); (312); (101) crystal planes and those interplanar distance of lattice spacing matched to the previous reports [22–24]. The determination of d-spacing considers to the Bragg's law, $\lambda = 2d\ sin\theta$, where $\lambda$ is X-ray wavelength with Cu Kα radiation, $d$ is interplane spacing, and $\theta$ is the Bragg angle. By using the Debye-Scherrer equation, $L = K\lambda/\beta Cos\theta$, we obtained the average crystallite value for $Bi_5O_7I$, which was 28.66 nm and 25 nm for $TiO_2$, whereas $L$ is the crystallite size, $K$ is the constant (0.9), $\lambda$ is X-ray wavelength with Cu Kα radiation (0.154 nm), $\beta$ is FWHM value, and $\theta$ is the Bragg angle. This result is near from to the calculated crystal size value in the previous work [25].

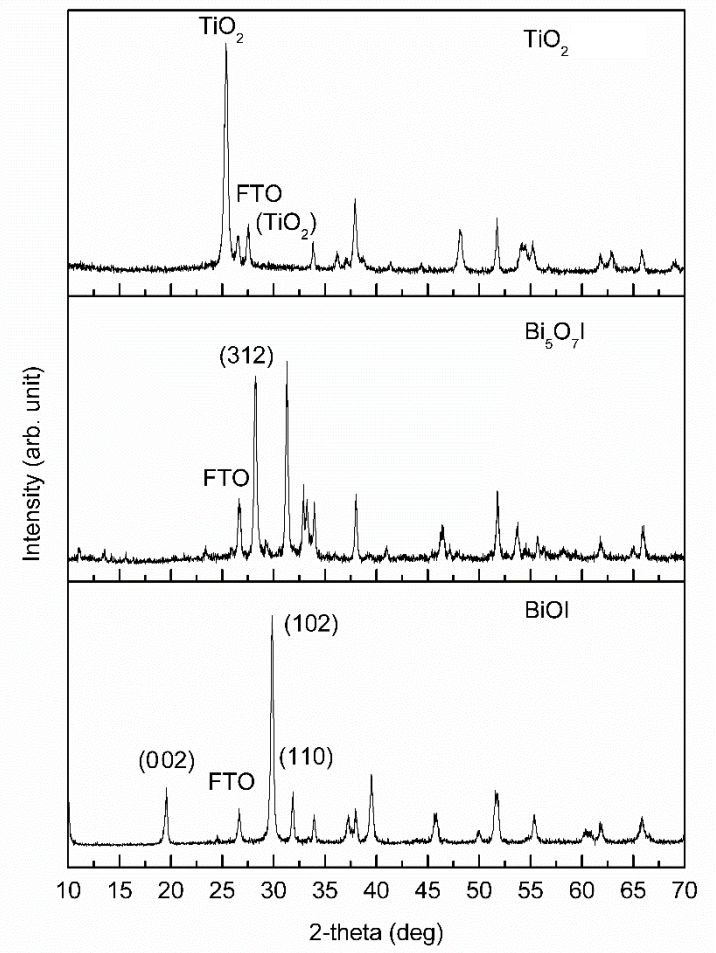


**Figure 1** Diffractogram of $TiO_2$, $Bi_5O_7I$, and BiOI.

Figure 2 displays the backscattered (BSE) SEM images of composited $TiO_2/Bi_5O_7I$ at the percentage of $Bi_5O_7I$ was 12.5% and 25%. The BSE images can depict the differences in composition of material clearly. It is obviously seen from the picture that the more $Bi_5O_7I$

percentage likes in Fig. 2B will show the more contained bigger material. The morphology of $TiO_2$ is particulate and $Bi_5O_7I$ is sheet-like shape. The sheet $Bi_5O_7I$ shape is a common morphology in the bismuth-based material since the (001) crystal plane is easy to form in the BiOI which depends on the amount of water as solvent during BiOI preparation [26]. Here we noticed that $Bi_5O_7I$ has the bigger size than $TiO_2$ which is in line to its crystallite size of both materials.

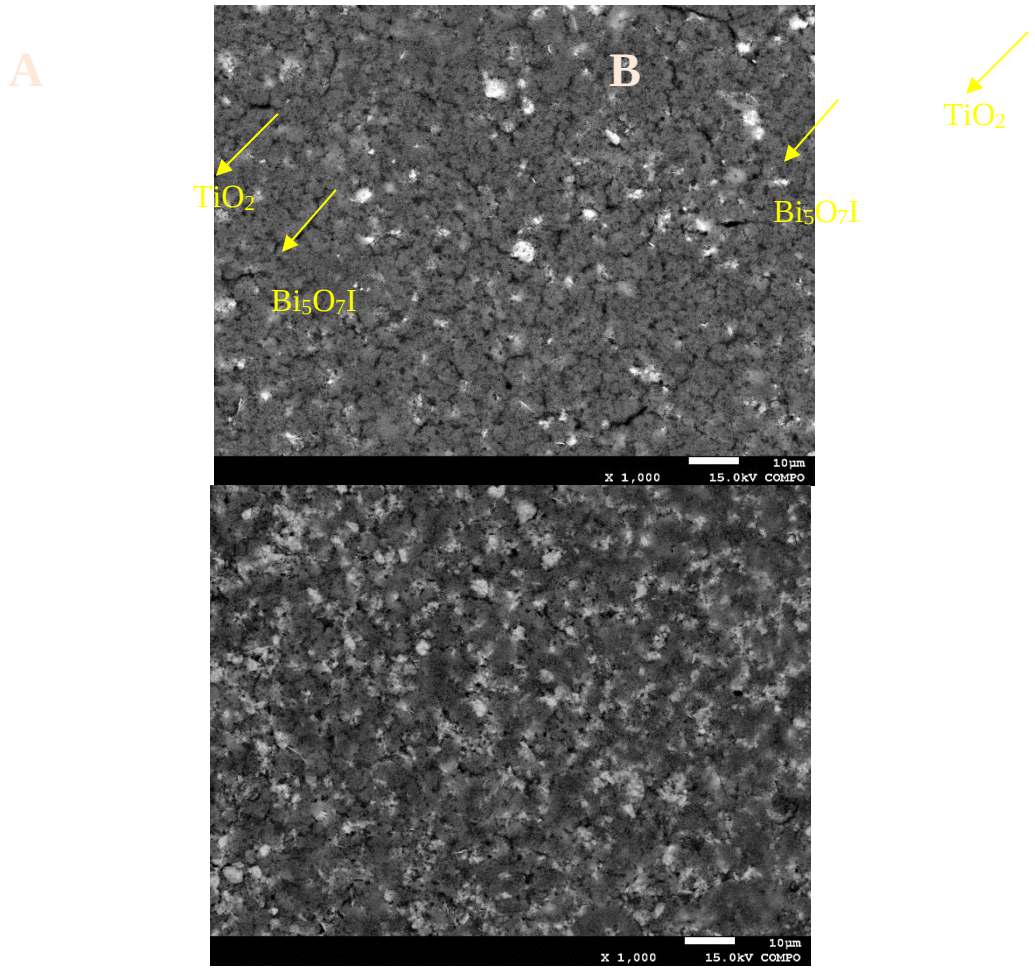

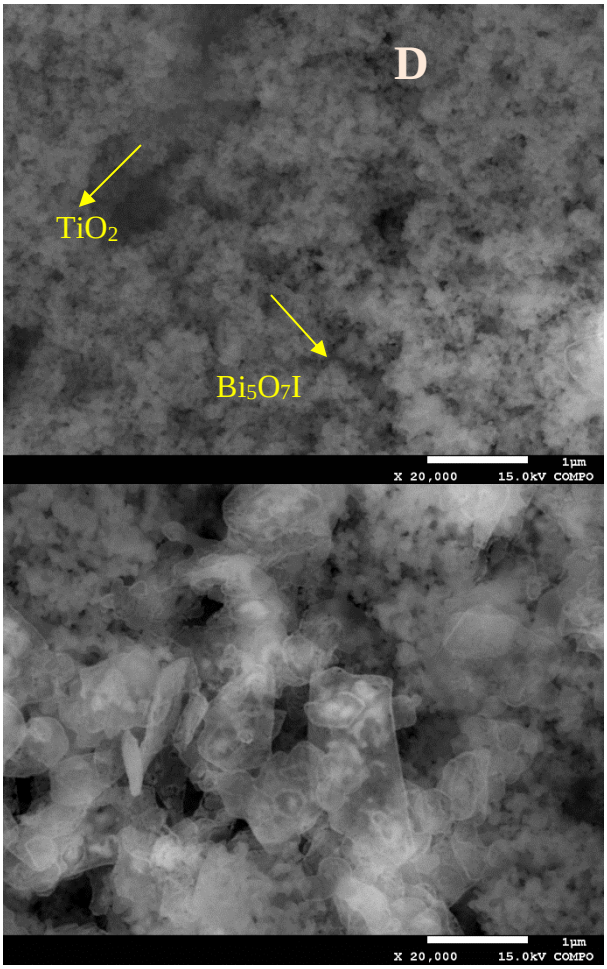


**Figure 2** Backscattered electron SEM images of 12.5% (A) and 25% (B) of $Bi_5O_7I$ and the higher magnification of 12.5% (C) and 25% films (D).

Analysis with UV-Visible spectroscopy resulted in the displayed graph in Fig. 3. It informs that owing to the higher mass percentage of $Bi_5O_7I$ in the composite films, it resulted in the slight red-shift behavior of material response under the visible light. However, during the experiment, we noticed that the opacity increased along with the increase in the amount of $Bi_5O_7I$. The band gap energy determination from Tauc plot calculation follows the indirect band gap model which the equation is $\alpha h\upsilon = A(h\upsilon - Eg)^{n/2}$. The coefficient of absorption, Planck constant, photonic frequency, band gap energy, and the value which is correlated to the semiconductor transition are notated: $\alpha$, $h$, $\upsilon$, $Eg$, $n$. $n=1$ is the transition model that is allowed as the indirect transition. We obtained the biggest band gap energy was more than 3 eV which came from the pure $TiO_2$. As the $Bi_5O_7I$ added, the decrease in its band gap energy has been detected. Therefore, we obtained the maximum wavelength absorption around 399 nm; 411 nm; 416 nm; 430 nm; and 490 nm for $Bi_5O_7I$ percentage in $TiO_2$/$Bi_5O_7I$ 0%; 6.25%; 12.5%; 25%; and 100%, respectively.

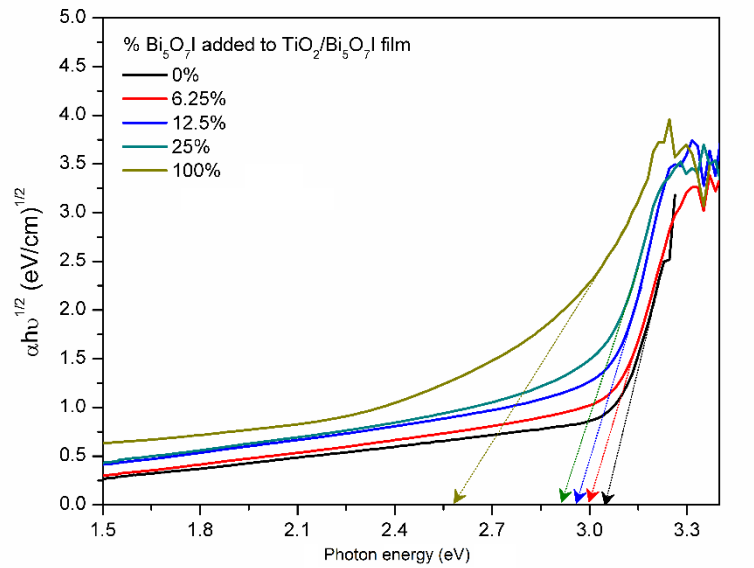


**Figure 3** Tauc plot of $TiO_2$; $TiO_2/Bi_5O_7I$; and $Bi_5O_7I$ films.

Study in the photovoltaic behavior for $TiO_2/Bi_5O_7I$ films was carried out using solar simulator system with Xenon lamp. The illustration of device is displayed in Fig. 4 and the I-V test result is shown in the Fig. 5A. A trend in the Jsc and Voc values is also shown in the Fig. 5B. By these results, we notice that the $Bi_5O_7I$ usage has an effect on its photovoltaic performance. As the amount of this material increases, the ability in light harvesting also increases. Therefore, its Jsc will be higher as the impact of the higher visible light absorption. Comparing to the pure $TiO_2$ film in $TiO_2/Bi_5O_7I$ 0%, the only $Bi_5O_7I$ photoanode exhibits the highest photovoltaic parameter due to its highest Jsc. In addition, the bigger size of $Bi_5O_7I$ may have the light scattering effect to maximize its Jsc. Therefore, the PCE has doubled for the $Bi_5O_7I$ device. The resulting composite material shows the quality improvement as the electronic conductor material which is indicated by the slight increment in the open-circuit voltage value and a gradual increase of the short-circuit current.

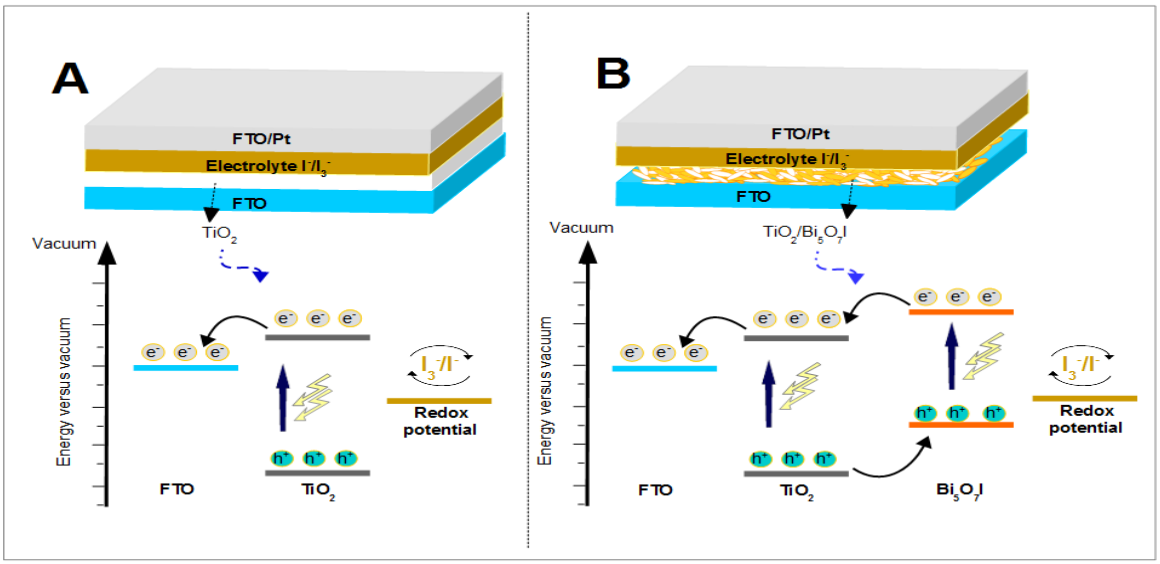


**Figure 4** The illustration of photovoltaic device structure for $TiO_2$ (A) and $TiO_2/Bi_5O_7I$ (B).

We have compared the $TiO_2/Bi_5O_7I$ cell with the $TiO_2/Bi_2O_3$ cell and $TiO_2$/BiOI cell from the previous reports. Due to the different band gap energy among those bismuth materials, with the arrangement: BiOI < $Bi_5O_7I$ < $Bi_2O_3$, the short-circuit current also has the order list: $TiO_2$/BiOI > $TiO_2/Bi_5O_7I$ > $TiO_2/Bi_2O_3$ [9,27]. Here we supposed that the light harvesting ability of those materials is responsible to short-circuit current enhancement. Generally, the more addition of $Bi_5O_7I$ to the films also has an impact on the open-circuit voltage (Voc). The new electronic structure due to the combination of $Bi_5O_7I$ and $TiO_2$ may be the reason on the Voc changing. It is clearly shown that by involving $Bi_5O_7I$, it can exhibit the better performance than pure $TiO_2$. The changing in its electronic state between in $TiO_2$ and composite $TiO_2/Bi_5O_7I$ films due to the $Bi_5O_7I$ addition resulted in the different band gap energy which is followed by the rearrangement in its Fermi level energy state. As a result, the recombination in the composited material might be lower in comparison to the $TiO_2$ itself. Thus, the Voc increases since the collected electron by FTO which travelled within the devices may be higher in the composite cell.

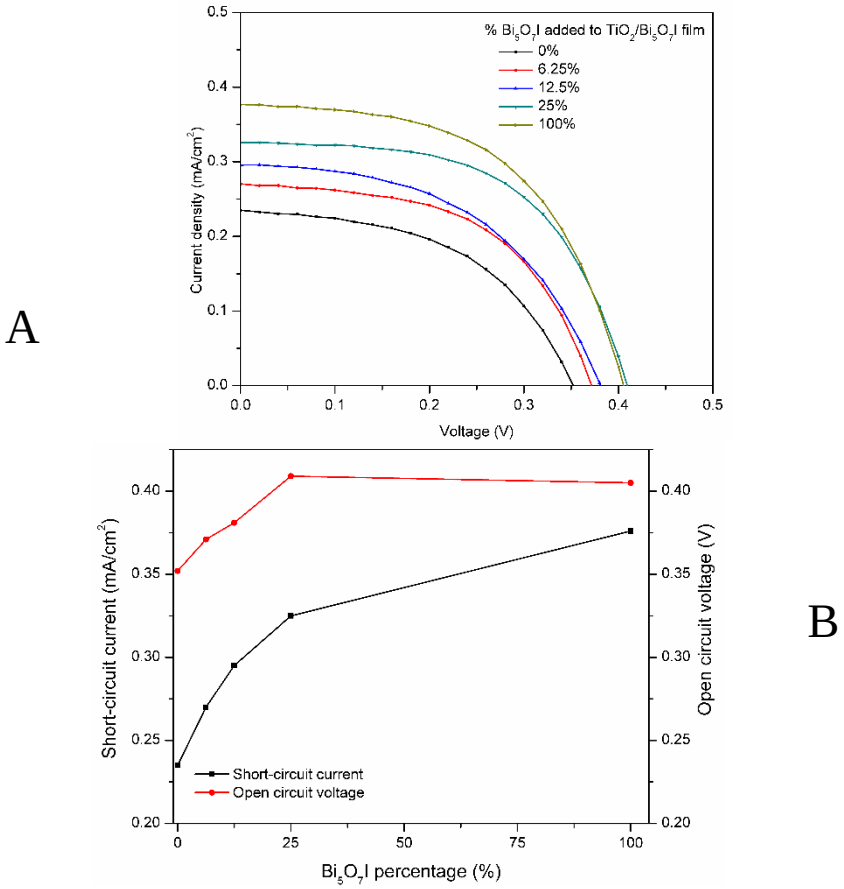


**Figure 5** I-V curve (A) and Jsc and Voc graph (B) of $TiO_2/Bi_5O_7I$ photovoltaic devices in the different percentage of $Bi_5O_7I$.

## 4. CONCLUSIONS

$TiO_2/Bi_5O_7I$ nanocomposite films have been successfully prepared by the annealing treatment of $TiO_2$/BiOI at 450 $^oC$. The annealing of BiOI could transform BiOI to $Bi_5O_7I$ without any detected impurities. A backscattered electron images by SEM analysis could show the blending of $TiO_2$ and $Bi_5O_7I$ in the sample. The greater number of bigger materials as $Bi_5O_7I$ in the SEM image could be an evident that the more amount of $Bi_5O_7I$ added to the sample. As the $Bi_5O_7I$ weight percentage increased, it could induce the red-shifting of composite materials which extended the visible absorption wavelength edge. Therefore, $Bi_5O_7I$ usage had the impact on its photovoltaic properties. By increasing the amount of $Bi_5O_7I$, it can be clearly observed that the Jsc increased and resulted in the higher PCE value. The changing in the film composition also could reveal the different Voc value which could be caused by the different electronic structure of semiconductor material in our photoanodes. This report shows that without employing the dye, $Bi_5O_7I$ can be used as the photoanode component for photovoltaic device and it achieved the better performance than the only $TiO_2$ film.

**References**

[1] P.K. Nayak, S. Mahesh, H.J. Snaith, D. Cahen, Nat. Rev. Mater. 4 (2019) 269
[2] C.P. Sajan, S. Wageh, A.A. Al-Ghamdi, J. Yu, S. Cao, Nano Res. 9 (2016) 3
[3] B. Kilic, S. Turkdogan, A. Astam, S.S. Baran, M. Asgin, E. Gur, Y. Kocak, J. Nanoparticle Res. 20 (2018) 11
[4] M.Y.A. Rahman, S.N. Sadikin, A.A. Umar, Appl. Phys. A Mater. Sci. Process. 124 (2018) 460
[5] X. Liu, Z. Xing, H. Zhang, W. Wang, Y. Zhang, Z. Li, X. Wu, X. Yu, W. Zhou, ChemSusChem 9 (2016) 1118
[6] P. Luan, M. Xie, X. Fu, Y. Qu, X. Sun, L. Jing, Phys. Chem. Chem. Phys. 17 (2015) 5043
[7] K. Du, G. Liu, X. Chen, K. Wang, J. Electrochem. Soc. 162 (2015) E251
[8] S. Shalini, R. Balasundaraprabhu, T. Satish Kumar, N. Prabavathy, S. Senthilarasu, S. Prasanna, Int. J. Energy Res. 40 (2016) 1303
[9] M. Chang, H. Hu, Y. Zhang, D. Chen, L. Wu, X. Li, Nanomaterials 7 (2017) 104
[10] S. Sun, W. Wang, L. Zhang, L. Zhou, W. Yin, M. Shang, Environ. Sci. Technol. 43 (2009) 2005
[11] J. Yang, L. Xu, C. Liu, T. Xie, Appl. Surf. Sci. 319 (2014) 265
[12] C. Liu, X.J. Wang, Dalt. Trans. 45 (2016) 7720
[13] X. Jiang, Y. Ma, C. Zhao, Y. Chen, M. Cui, J. Yu, Y. Wu, Y. He, J. Mater. Res. 33 (2018) 2385
[14] W.L. Huang, Q. Zhu, J. Comput. Chem. 30 (2009) 183
[15] Y. Li, H. Yao, J. Wang, N. Wang, Z. Li, Mater. Res. Bull. 46 (2011) 292
[16] A. Kudo, K. Omori, H. Kato, J. Am. Chem. Soc. 121 (1999) 11459
[17] X. Xiao, C. Xing, G. He, X. Zuo, J. Nan, L. Wang, Appl. Catal. B Environ. 148–149 (2014) 154
[18] A.A. Putri, S. Kato, N. Kishi, T. Soga, Jpn. J. Appl. Phys. 58 (2019) 9
[19] H. Wang, L. Xu, C. Liu, Y. Lu, Q. Feng, T. Wu, R. Wang, Nanomaterials 9 (2019) 118
[20] W.K. Wang, J.J. Chen, X. Zhang, Y.X. Huang, W.W. Li, H.Q. Yu, Sci. Rep. 6 (2016) 665
[21] P. Selvaraj, A. Roy, H. Ullah, P. Sujatha Devi, A.A. Tahir, T.K. Mallick, S. Sundaram, Int. J. Energy Res. 43 (2019) 523
[22] M. Mourad Mabrook, Exp. Theo. NANOTECHNOLOGY 2 (2018) 103
[23] L.A. Mabuti, I.K.S. Manding, C.C. Mercado, RSC Adv. 8 (2018) 42254
[24] Z. Zhao, W. Zhang, X. Lv, Y. Sun, F. Dong, Y. Zhang, Environ. Sci. Nano 3 (2016) 1306
[25] H. Feng, X. Jiao, R. Chen, X. Zhu, Q. Liao, D. Ye, B. Zhang, W. Zhang, J. Power Sources 419 (2019) 162
[26] J. Lu, J. Wu, W. Xu, H. Cheng, X. Qi, Q. Li, Y. Zhang, Y. Guan, Y. Ling, Z. Zhang, Mater. Lett. 219 (2018) 260
[27] S. Sfaelou, D. Raptis, V. Dracopoulos, P. Lianos, RSC Adv. 5 (2015) 95813